STOCHASTIC TEMPORAL PROPERTIES OF THE SASE FEL*

S. Krinsky#, BNL, Upton, NY 11973, U.S.A.

Abstract

We review the statistical description of the chaotic time evolution of the radiation from a self-amplified spontaneous-emission free-electron laser in the linear region before saturation.

INTRODUCTION

A high-gain, self-amplified spontaneous-emission (SASE) free-electron laser (FEL) [1, 2], based on modern beam technology, has the advantage of operating without a resonator and hence is capable of generating coherent radiation with wavelength down to the x-ray region. The LCLS at SLAC has recently achieved high gain and saturation at 1.5 Å [3]. A review of SASE theory can be found in ref. [4].

The gain in an FEL is based on the constructive growth of a microbunching instability in an electron beam, which grows as the result of an interaction between the electron beam and the electromagnetic wave it emits as it traverses the magnetic field of the undulator. The instability modulates the electron density on the scale of the radiation wavelength resulting in coherent radiation. Provided that the instability is strong enough, the radiation grows exponentially before reaching saturation. The wavelength of an FEL is determined by the resonance frequency

$$\omega_r = \frac{4\pi c\gamma^2}{\lambda_w(1+a_w^2)}. \qquad (1)$$

Here γ is the relativistic factor of the beam, and λ_w and a_w are respectively the undulator period and rms field strength parameter.

The SASE FEL starts up from the shot noise in the electron beam [5-7]. The temporal behavior of the system is that of a narrow-band amplifier with a broadband Poisson seed. Before saturation the output is a Gaussian random process and the radiated field is chaotic, quasi-monochromatic, polarized light. Near saturation, the transverse behavior of the output is dominated by an intense, single spatial mode. Ignoring the transverse dependence, the radiated electric field can be expressed in the form

$$E(z,t) = A(z,t)\exp(ik_r z - i\omega_r t), \qquad (2)$$

where z represents the location along the undulator at which the SASE is observed and t represents the temporal position in the radiation pulse. The SASE field before saturation is the superposition of many electromagnetic wave packets emitted from randomly distributed, individual electrons. Within the classical, one-dimensional theory, the slowly varying envelope can be approximated by

$$A(z,t) \cong A_0(z)\sum_{j=1}^{N_e}\exp\left[i\omega_r t_j - \frac{(t-t_j-z/v_g)^2}{4\sigma^2}\left(1+\frac{i}{\sqrt{3}}\right)\right], \qquad (3)$$

where N_e is the total number of electrons in the bunch, $A_0(z)$ contains the exponential growth factor, t_j is the random arrival time of the j^{th} electron at the undulator entrance, and $v_g = \omega_r / \left(k_r + \frac{2}{3}k_w\right)$. The wave packet width $\sigma = 1/(\sqrt{3}\,\sigma_\omega)$, where $\sigma_\omega = \omega_r\sqrt{3\sqrt{3}\rho/k_w z}$ is the SASE bandwidth [5,6] and ρ the FEL Pierce parameter [2].

STATISTICAL DESCRIPTION

Overview

To describe the shot noise, one considers the arrival time of the individual electrons at the undulator entrance to be independent random variables, and determines the statistical properties of the output radiation by averaging over the stochastic ensemble of arrival times. In the linear regime before saturation, the Central Limit Theorem implies that the probability distribution for the spectral intensity $\tilde{I}(\omega)$, or the time-domain intensity $I(t)$, is the negative exponential distribution [8-11]

$$p_I(I) = \frac{1}{\langle I\rangle}e^{-I/\langle I\rangle}, \qquad (4)$$

and the intensity fluctuation is 100%. The bracket indicates an ensemble average over the arrival times.

The output intensity as a function of time exhibits spiking [12] (see Fig. 1a), and the width of the intensity peaks is characterized by the coherence time [8-16], $T_{coh} = \sqrt{\pi}/\sigma_\omega$, where σ_ω is the SASE gain bandwidth. The spectral intensity also exhibits spikes (Fig. 1b), and the width of the spectral peaks is inversely proportional to the pulse duration.

At a fixed position z along the undulator, consider the energy in a single SASE pulse,

$$W(z) \propto \int |E(t,z)|^2\, dt\ . \qquad (5)$$

For z fixed, one can think of dividing the pulse into M statistically independent time-intervals of width T_{coh}. The energy fluctuation within a single coherent region is 100%, but the fluctuation σ_W/W of the energy in the entire pulse is reduced [8-11,14],

$$\frac{\sigma_W^2}{W^2} = \frac{(W-\langle W\rangle)^2}{\langle W\rangle^2} = \frac{1}{M} = \frac{T_{coh}}{T_b}. \qquad (6)$$

*Work supported by DOE contract DE-AC02-98CH10886.

#krinsky@bnl.gov

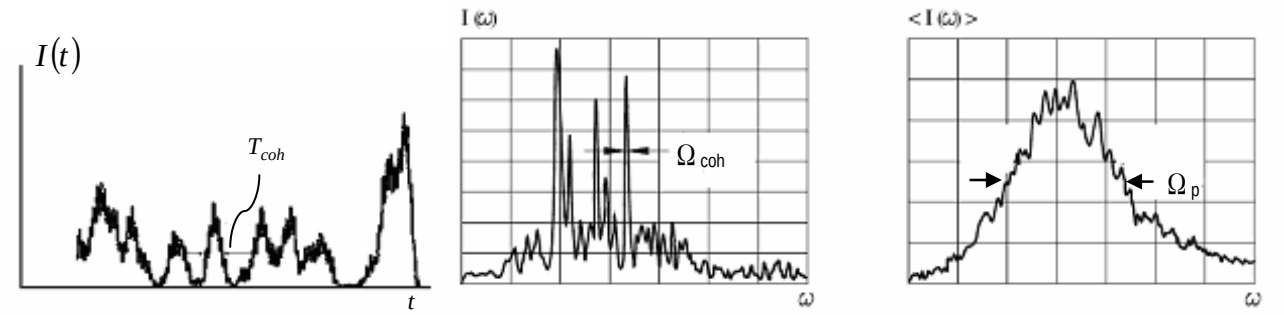

(a) (b) (c)

Figure 1: (a) Intensity spiking in the time-domain. Width of peaks is characterized by the coherence time T_{coh} (b) Intensity spiking in the frequency-domain. Width of spectral peaks Ω_{coh} inversely proportional to pulse length. (c) Average spectrum of many SASE pulses. Spectral width Ω_p inversely proportional to the coherence time.

The energy per pulse is described approximately by the gamma distribution [8-11],

$$p_W(W) = \frac{M^M}{\Gamma(M)}\left(\frac{W}{\langle W\rangle}\right)^{M-1}\frac{1}{\langle W\rangle}\exp\left(-M\frac{W}{\langle W\rangle}\right). \quad (7)$$

For an unchirped Gaussian pulse of rms duration $\sigma_t > T_{coh}$, Table 1 provides useful guidance [16]:

Table 1: Approximate description of SASE statistics.

Number of modes	$M \cong 2\sigma_t\,\sigma_\omega$
Pulse duration	$T_p \equiv 2\sqrt{\pi}\,\sigma_t$
Coherence time	$T_{coh} \equiv T_p / M \cong \sqrt{\pi}/\sigma_\omega$
Temporal spike rms width	$\langle \delta t\rangle \cong T_{coh}/\sqrt{2\pi}$
Temporal spike separation	$\langle \Delta t\rangle \cong \sqrt{2\pi}/\sigma_\omega$
Spectral width	$\Omega_p \equiv 2\sqrt{\pi}\,\sigma_\omega$
Range spectral coherence	$\Omega_{coh} \equiv \Omega_p / M \cong \sqrt{\pi}/\sigma_t$
Frequency rms spike width	$\langle \delta\omega\rangle \cong \Omega_{coh}/\sqrt{2\pi}$
Frequency spike separation	$\langle \Delta\omega\rangle \cong \sqrt{2\pi}/\sigma_t$

Mathematical Formalism

The mathematical formalism presented here is valid for a general random process E(t) with $\langle E(t)\rangle = 0$. It need be neither stationary nor Gaussian. The Wigner function [17], defined by

$$W(t,\omega) \equiv \int d\tau \left\langle E\left(t-\frac{\tau}{2}\right)E^*\left(t+\frac{\tau}{2}\right)\right\rangle \exp(-i\omega\tau), \quad (8)$$

has many of the properties of a phase space density, although it can take negative values. Integrating the Wigner function over frequency, we obtain the average instantaneous intensity,

$$\left\langle |E(t)|^2\right\rangle = \int \frac{d\omega}{2\pi} W(t,\omega) \quad (9)$$

and integrating over time, the average spectral intensity

$$\left\langle \left|\tilde{E}(\omega)\right|^2\right\rangle = \int dt\, W(t,\omega). \quad (10)$$

The number of temporal modes M in a radiation pulse should be equal to the ratio of the area of the time-frequency phase space it occupies divided by the minimum required phase space area. With this in mind, the number of modes M can be expressed in terms of the Wigner function via,

$$\frac{1}{M} \equiv \frac{\int \frac{dtd\omega}{2\pi} W^2(t,\omega)}{\left(\int \frac{dtd\omega}{2\pi} W(t,\omega)\right)^2}. \quad (11)$$

Working in the time domain, Eq. (11) can be written in the form [9]

$$\frac{1}{M} = \frac{\int dt_1 dt_2 \left|\langle E(t_1)E^*(t_2)\rangle\right|^2}{W^2}, \quad (12)$$

where the integrated intensity W is given by

$$W = \int \frac{dtd\omega}{2\pi} W(t,\omega) = \int dt \left\langle |E(t)|^2\right\rangle. \quad (13)$$

The Schwartz inequality implies $M \geq 1$.

Let us define the radiation pulse duration T_p by

$$\frac{1}{T_p} \equiv \frac{\int dt \left\langle |E(t)|^2\right\rangle^2}{\left(\int dt \left\langle |E(t)|^2\right\rangle\right)^2}, \quad (14)$$

and define the coherence time T_{coh} by

$$T_{coh} \equiv T_p / M. \quad (15)$$

It follows from (12), (14) and (15) that

$$T_{coh} = \frac{\int dt_1 dt_2 \left|\langle E(t_1)E^*(t_2)\rangle\right|^2}{\int dt \left\langle |E(t)|^2\right\rangle^2}. \quad (16)$$

Working in the frequency domain, we can express the number of modes as,

$$\frac{1}{M}=\frac{\int \frac{d\omega_1}{2\pi}\frac{d\omega_2}{2\pi}\left|\left\langle \tilde{E}(\omega_1)\tilde{E}(\omega_2)\right\rangle\right|^2}{W^2}. \quad (17)$$

We define the spectral width Ω_p of the pulse by

$$\frac{1}{\Omega_p}\equiv\frac{\int d\omega\left\langle\left|\tilde{E}(\omega)\right|^2\right\rangle^2}{\left(\int d\omega\left\langle\left|\tilde{E}(\omega)\right|^2\right\rangle\right)^2} \quad (18)$$

and the range of spectral coherence by

$$\Omega_{coh}\equiv\Omega_p/M. \quad (19)$$

Then the range of spectral coherence is given by

$$\Omega_{coh}=\frac{\int d\omega_1 d\omega_2\left|\left\langle \tilde{E}(\omega_1)\tilde{E}^*(\omega_2)\right\rangle\right|^2}{\int d\omega\left\langle\left|\tilde{E}(\omega)\right|^2\right\rangle^2}. \quad (20)$$

The fluctuation of the integrated intensity σ_W is

$$\sigma_W^2=\int dt_1 dt_2\left[\left\langle|E(t_1)|^2|E(t_2)|^2\right\rangle-\left\langle|E(t_1)|^2\right\rangle\left\langle|E(t_2)|^2\right\rangle\right]. \quad (21)$$

For a Gaussian random process with zero mean [8-11],

$$\left|\left\langle E(t_1)E^*(t_2)\right\rangle\right|^2=\left\langle|E(t_1)|^2|E(t_2)|^2\right\rangle-\left\langle|E(t_1)|^2\right\rangle\left\langle|E(t_2)|^2\right\rangle. \quad (22)$$

In this special case, valid for SASE in the linear regime before saturation, it follows from Eqs. (11,21,22) that

$$\frac{\sigma_W^2}{W^2}=\frac{1}{M}. \quad (23)$$

Simplified Model of SASE Pulse

A full treatment of SASE from a Gaussian bunch would take into account the dependence of the FEL gain on the electron density profile, which results in a dependence of the wave packet duration σ [Eq. (3)] on the temporal position in the pulse. Here, we shall ignore this dependence and consider constant σ.

We suppose the electron bunch to have a Gaussian average density profile

$$w_b(t)=\frac{1}{\sqrt{2\pi}\,\sigma_b}\exp\left(-t^2/2\sigma_b^2\right), \quad (24)$$

and consider the time dependence of the SASE amplitude (2) observed at a fixed position z. Suppressing the dependence on z, we write the complex, slowly varying amplitude in the linear region before saturation as

$$A(t)=A_0\sum_{j=1}^{N_e}\exp\left(\frac{-\chi\left(t-t_j\right)^2}{4\sigma^2}+i\omega_r t_j\right), \quad (25)$$

where $\chi=1+i\kappa$ with $\kappa=1/\sqrt{3}$. The times t_j are randomly distributed according to the Gaussian distribution $w_b(t)$ of Eq. (24). We assume that $\omega_r\sigma_b$ & $\omega_r\sigma >>1$, so $\langle A(t)\rangle\approx 0$. Averaging over the stochastic ensemble, we find the correlation function [16] $\langle A(t_1)A^*(t_2)\rangle=$

$$\frac{N_e\sigma A_0^2}{\sqrt{\sigma_b^2+\sigma^2}}\exp\left(\frac{-\left(1+\kappa^2\right)\sigma_b^2(t_1-t_2)^2-2\sigma^2\left(\chi t_1^2+\chi^* t_2^2\right)}{8\left(\sigma_b^2+\sigma^2\right)\sigma^2}\right) \quad (26)$$

and the Wigner function [16],

$$W(t,\omega)=\frac{N_e\sigma A_0^2\sqrt{2\pi}}{\sigma_t\sigma_{\omega 0}}\exp\left(-\frac{t^2}{2\sigma_t^2}-\frac{(\omega-\omega_r-\mu t)^2}{2\sigma_{\omega 0}^2}\right), \quad (27)$$

where,

$$\sigma_t^2=\sigma_b^2+\sigma^2,\ \sigma_{\omega 0}^2=\frac{1+\kappa^2}{4\sigma^2}-\frac{\kappa^2}{4\sigma_t^2},\ \mu=\frac{\kappa}{2\sigma_t^2}. \quad (28)$$

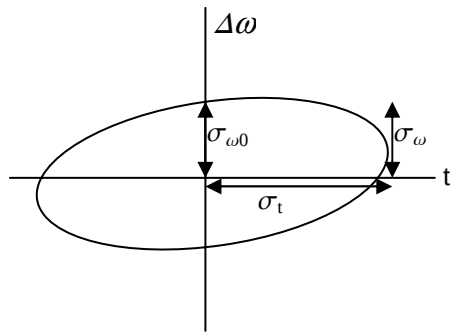

Figure 2: Region of phase space occupied by radiation. $\Delta\omega=\omega-\omega_r$. Area is $2\pi\sigma_t\sigma_{\omega 0}$.

Integrating the Wigner function over frequency we obtain the average instantaneous intensity,

$$\int\frac{d\omega}{2\pi}W(t,\omega)=\frac{N_e\sigma A_0^2}{\sigma_t}\exp\left(-t^2/2\sigma_t^2\right), \quad (29)$$

and integrating over time, the average spectral intensity

$$\int dt\,W(t,\omega)=\frac{2\pi N_e\sigma A_0^2}{\sigma_\omega}\exp\left[-(\omega-\omega_r)^2/2\sigma_\omega^2\right]. \quad (30)$$

It is seen that the rms radiation bandwidth is given by

$$\sigma_\omega^2=\sigma_{\omega 0}^2+\mu^2\sigma_t^2=\left(1+\kappa^2\right)/4\sigma^2. \quad (31)$$

In ref. [16], the results in Table 2 are derived.

Table 2: Statistical properties in model.

Number of modes	$M=2\sigma_t\,\sigma_{\omega 0}=\sqrt{4\sigma_b^2\,\sigma_\omega^2+1}$
Pulse energy fluctuation	$\sigma_W/W=1/\sqrt{M}$
Pulse duration	$T_p=2\sqrt{\pi}\,\sigma_t$
Coherence time	$T_{coh}=T_p/M=\sqrt{\pi}/\sigma_{\omega 0}$
Spectral width	$\Omega_p=2\sqrt{\pi}\,\sigma_\omega$
Range of spectral coherence	$\Omega_{coh}=\frac{\Omega_p}{M}=\sqrt{\frac{\pi}{\sigma_b^2+\frac{1}{4\sigma_\omega^2}}}$

FREQUENCY CHIRPED SASE

Characterization

Consider an electron beam passing through an undulator having period $\lambda_w = 2\pi/k_w$ and rms field strength parameter a_w. The j^{th} electron has energy γ_j (in units of its rest mass), average longitudinal velocity $v_j \cong c\left(1-\frac{1+a_w^2}{2\gamma_j^2}\right)$, and arrives at the undulator entrance at time t_j. We suppose the electron beam energy to have a linear chirp [18-21] α specified by

$$\frac{\gamma_j-\gamma_0}{\gamma_0} = \alpha\frac{t_j}{T_b}, \tag{32}$$

where T_b is the full temporal width of the uniform density electron pulse and ct_j is the longitudinal deviation from the beam center $t_j = 0$. From Eq. (1), we see that the energy chirp gives rise to a linear frequency chirp

$$\omega_j = \omega_0 + ut_j, \tag{33}$$

where $u = 2\alpha\omega_0/T_b$.

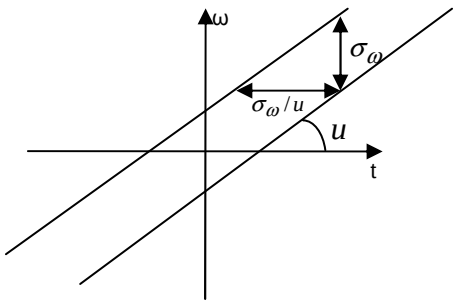

Figure 3: Time-frequency phase space for chirped radiation.

In the exponential growth regime before saturation, the SASE electric field has the form

$$E(z,t) \propto \sum_{j=1}^{N_e} e^{ik_j z - i\omega_j(t-t_j)} g(z, t-t_j; u), \tag{34}$$

where the green's function can be approximated by [21],

$$g(z,t-t_j;u) \cong e^{\rho(\sqrt{3}+i)k_w z} e^{-b\left(t-t_j-\frac{z}{v_g}\right)^2} e^{-\frac{iu}{2}\left(t-t_j-\frac{z}{v_0}\right)\left(t-t_j-\frac{z}{c}\right)}. \tag{35}$$

The wave number of radiation from the j^{th} electron is

$$k_j = \frac{\omega_j}{c} = k_w\left(\frac{v_j}{c-v_j}\right) \cong \frac{2\gamma_j^2 k_w}{1+a_w^2}. \tag{36}$$

The complex parameter b is defined by

$$b = \frac{3}{4}\left(1+\frac{i}{\sqrt{3}}\right)\sigma_\omega^2. \tag{37}$$

To analyze the statistical properties of the chirped SASE output, we consider the arrival times t_j to be random variables and average over the uniform stochastic ensemble. The time correlation function is [21]

$$\left\langle E\left(z,t-\frac{\tau}{2}\right)E^*\left(z,t+\frac{\tau}{2}\right)\right\rangle \propto e^{2\rho\sqrt{3}k_w z} e^{\frac{-iu\tau}{2}\left(\frac{z}{v_0}+\frac{z}{c}\right)} e^{i(\omega_0+ut)\tau} e^{-\sigma_\omega^2\tau^2/2}. \tag{38}$$

We find the coherence time

$$T_{coh} = \sqrt{\pi}/\sigma_\omega, \tag{39}$$

and the number of modes in the chirped radiation pulse

$$M \equiv T_b/T_{coh} = \sigma_\omega T_b/\sqrt{\pi}, \tag{40}$$

are independent of the energy chirp.

The frequency correlation function is [21]

$$\left\langle \tilde{E}\left(z,\omega-\frac{\Omega}{2}\right)\tilde{E}^*\left(z,\omega+\frac{\Omega}{2}\right)\right\rangle \propto e^{2\rho\sqrt{3}k_w z} e^{\frac{i\Omega}{2}\left(\frac{z}{v_0}+\frac{z}{c}\right)} e^{-i(\omega-\omega_0)\frac{\Omega}{u}} e^{-\frac{\sigma_\omega^2\Omega^2}{2u^2}} \tag{41}$$

and the range of spectral coherence

$$\Omega_{coh} = |u|T_b/M = |u|T_{coh}. \tag{42}$$

In the absence of the frequency chirp, $\Omega_{coh} = 2\pi/T_b$. In this paper, when we consider a chirped electron beam, we assume that $|u|T_{coh} >> 2\pi/T_b$.

The Wigner function is given by [21]

$$W(z;t,\omega) \propto e^{2\rho\sqrt{3}k_w z} \exp\left(-\frac{1}{2\sigma_\omega^2}\left[\omega-\omega_0-u\left(t-\frac{1}{2}\left(\frac{z}{v_0}+\frac{z}{c}\right)\right)\right]^2\right). \tag{43}$$

Pulse Slicing Using Monochromator

One can use a monochromator to select a short portion of the frequency chirped radiation pulse [19,20]. In order to investigate the properties of such filtered output, let us assume that the electric field $E_F(t,z)$ after the monochromator has the form

$$E_F(z,t) = \int \frac{d\omega}{2\pi} e^{-i\omega t}\,\tilde{E}(z,\omega)\,\exp\left[-\frac{(\omega-\omega_m)^2}{4\sigma_m^2}\right], \tag{44}$$

where $\tilde{E}(\omega,z)$ is the Fourier component of the electric field before the filter. The time-correlation function of the filtered radiation is [21]

$$\left\langle E_F\left(z,t-\frac{\tau}{2}\right)E_F{}^*\left(z,t+\frac{\tau}{2}\right)\right\rangle \propto e^{2\rho\sqrt{3}k_w z} e^{i\omega_m\tau} e^{-\frac{\sigma_m^2\tau^2}{2}} e^{-\frac{\left(t-t_m(z)-i\frac{\sigma_m^2\tau}{u}\right)^2}{2\sigma_t^2}}, \tag{45}$$

where

$$t_m(z) = \frac{\omega_m-\omega_0}{u} + \frac{1}{2}\left(\frac{z}{v_0}+\frac{z}{c}\right). \tag{46}$$

The pulse duration is characterized by the rms width σ_t given by [21]

$$\sigma_t^2 = \frac{\sigma_\omega^2 + \sigma_m^2}{u^2} + \frac{1}{4\sigma_m^2}. \quad (47)$$

It is seen that the pulse duration cannot be made smaller than $\sigma_\omega / |u|$, which is also apparent from the phase space geometry shown in Fig. 3. The last term in Eq. (47) assures that the filtered pulse cannot be shorter than the Fourier transform limit. The minimum pulse duration is obtained for monochromator bandwidth

$$\frac{\sigma_m}{\omega_0} = \sqrt{\frac{|u|}{2\omega_0^2}}. \quad (48)$$

This corresponds to a minimum rms pulse duration,

$$(\sigma_t)_{\min} = \sqrt{\frac{\sigma_\omega^2 + |u|}{u^2}}. \quad (49)$$

The energy fluctuation after the monochrometer is

$$\frac{\sigma_W}{W} = \frac{1}{\sqrt{M_F}}, \quad (50)$$

where the number of modes is given by [21]

$$M_F = \sqrt{\frac{4\sigma_m^2 \sigma_\omega^2}{u^2} + 1}. \quad (51)$$

The coherence time of the monochromated pulse is

$$T_{coh} = \frac{2\sqrt{\pi}\,\sigma_t}{M_F}, \quad (52)$$

and the range of spectral coherence is

$$\Omega_{coh} = \frac{2\sqrt{\pi}\,\sigma_m}{M_F}. \quad (53)$$

CENTRAL LIMIT THEOREM

The central limit theorem [8] states that the distribution P(V) of the normalized sum $V = (r_1 + r_2 + \cdots + r_N)/\sqrt{N}$ of N independent random vectors approaches the normal law as $N \to \infty$. For simplicity consider $\langle r_j \rangle = 0$; then as $N \to \infty$,

$$P(V) \to (2\pi)^{-K/2} (\det M)^{-1/2} \exp\left(-\frac{1}{2} V^T M^{-1} V\right), \quad (54)$$

where $V^T = (V_1, ..., V_K)$ is a K-dimensional row-vector (the superscript T indicates transpose) and V the corresponding column vector. The symmetric matrix M is comprised of the second moments:

$$M = \begin{bmatrix} \mu_{11} & \mu_{12} \cdots \mu_{1K} \\ \vdots & \\ \mu_{K1} & \mu_{K2} \cdots \mu_{KK} \end{bmatrix} \quad (55)$$

where

$$\mu_{jk} = \langle V_j V_k \rangle = \int d^K V \, (V_j V_k) \, P(V). \quad (56)$$

M^{-1} is the inverse of the matrix M. Note that when the central limit theorem applies, the distribution is Gaussian and hence is determined by the second moments. Under these conditions, one need not compute all the higher moments to determine the distribution—a great simplification.

It is well-known that by choosing $V = [A(t), A^*(t)]$ one can show [8-11] that the distribution of the normalized intensity $Q = I/\langle I \rangle$ is given by the exponential distribution $P(Q) = \exp(-Q)$ as noted in Eq. (4). It is probably less widely known that by following Rice [8], one can use the central limit theorem to determine the probability distribution for intensity extrema. In this case, for a stationary Gaussian process, one selects $V = [A(t), A^*(t), A'(t), A'^*(t), A''(t), A'^*(t)]$, where prime denotes derivative with respect to time. Introducing the amplitude $R(t)$ and phase $\phi(t)$ via

$$A(t) / \sqrt{\langle |A(t)|^2 \rangle} = R(t) e^{i\phi(t)}, \quad (57)$$

define the normalized variables,

$$\rho = \frac{R}{\sqrt{2}}, \quad \eta = \frac{-R''}{\sigma_\omega^2 \sqrt{2}}, \quad \nu = \frac{\phi'}{\sigma_\omega}, \quad \mu = \frac{\phi''}{\sigma_\omega^2}. \quad (58)$$

Rice [8] has shown that the probability $p(\rho, \eta, \nu, \mu) d\rho\, d\eta\, d\nu\, d\mu\, dt$ of finding an extremum of intensity in the interval $d\rho\, d\eta\, d\nu\, d\mu\, dt$ is given by

$$p(\rho, \eta, \nu, \mu) = \frac{8\sigma_\omega}{\pi^2} |\eta| \rho^3 \exp\left(-3\rho^2 + 2\eta\rho - \left(\eta + \nu^2 \rho\right)^2 - \rho^2 \mu^2\right) \quad (59)$$

Maxima correspond to $\eta > 0$ and minima to $\eta < 0$. More details of the derivation can be found in ref. [8,16]. Integrating over ρ, η, ν, μ, one finds that the number of spikes per unit time is $1/\langle \Delta t \rangle \cong \sigma_\omega / \sqrt{2\pi}$. Carrying out integrations over specific subsets of variables, one can derive useful distributions characterizing peak height, width, and local phase derivative at the points of maximum (or minimum) intensity [8,16]. Some of these results have been compared to experiment at LEUTL [22,23].

FROG MEASUREMENTS AT LEUTL

At LEUTL [22,23], frequency resolved optical gating (FROG) [24] was used to characterize the temporal evolution of the chaotic SASE output, and the experimental results were found to be in agreement with the predictions of analytic theory as well as numerical simulation.

As illustrated in Fig. 4, the FEL output intensity as a function of time exhibits spiking. The width of the intensity spikes is characterized by the coherence time. We note that the phase change is small near the intensity maxima but can be larger near the intensity minima. The rapid phase variation at the minima is closely related to the loss of temporal coherence between spikes.

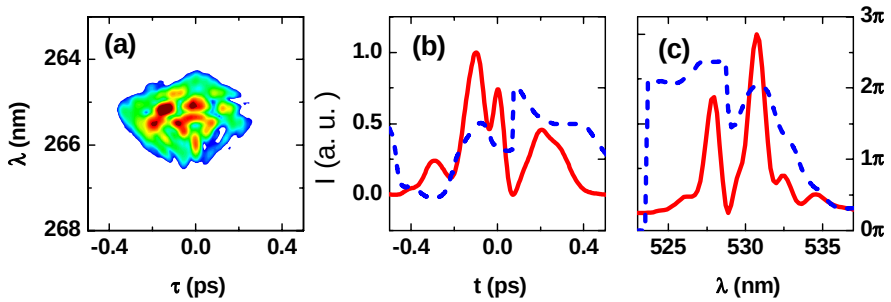

Figure 4: (a) Typical raw FROG data and the retrieved field intensity (red, solid) and phase (blue, dashed) as a function of time (b) and wavelength (c) of the SASE output. See ref. [22].

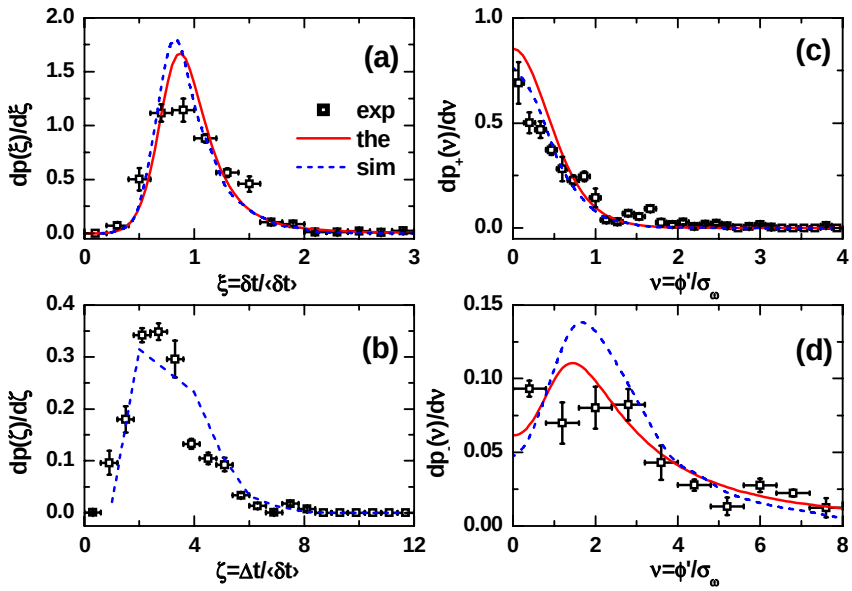

Figure 5: Distribution of (a) the spike width δt and (b) the peak-to-peak spacing Δt between the intensity spikes normalized to the average spike width $\langle \delta t \rangle$, phase derivative at the intensity maxima (c) and minima (d) normalized to the rms SASE FEL bandwidth. Experimental data (symbols), theoretical calculation (solid line) and simulation results (dashed lines) are all presented when possible. Note different horizontal scales for (c) and (d). See ref. [22].

Each FROG image and its retrieval shows a full characterization of the pulse, including the field phase and amplitude. Study of the shot-to-shot variation of multiple pulses provides the information on the statistics of the chaotic optical field.

Let us consider the time domain intensity spikes. We let δt denote the rms spike width and Δt the peak-to-peak spike separation. In Figs. 5 (a) and (b), we show the probability distributions of the normalized rms spike width $\xi = \delta t / \langle \delta t \rangle$ and the normalized spacing between the intensity maxima $\zeta = \Delta t / \langle \delta t \rangle$. For the ensemble of the pulses measured, $\langle \delta t \rangle = 52\, fs$ is the average value of the rms spike width. In Fig. 5 a, the distribution of the spike widths has a peak at a value slightly smaller than the average. It has a long tail extending to larger spike width and an abrupt drop at smaller spike width. The distribution in Fig. 5b for the spike spacing peaks at about $\Delta t / \langle \delta t \rangle = 3.0$, and its average is 3.25, in reasonable agreement with theory for a totally chaotic optical field, $\langle \Delta t \rangle / \langle \delta t \rangle = \left(\sqrt{2\pi} / \sigma_\omega\right) / \left(1/\sqrt{2}\sigma_\omega\right) = 2\sqrt{\pi} \cong 3.5$. Also shown in Figs. 5 (a) and (b), are the results of the numerical simulation (dashed lines) and analytic theory [16] solid lines.

Intuitively, since an individual intensity spike corresponds to a coherent region, the phase within the spike is expected to be correlated. On the other hand, due

to the lack of communication between different coherence regions, there can be a phase jump in the transition region between two spikes, as illustrated in Fig. 4. This phase behavior was quantified by measuring the time derivative of the phase (ϕ') of the slowly varying envelope at the intensity maxima and minima. The measured distributions (symbols) are presented in Figs. 5 (c) and (d), which show that indeed the phase drift rate is small at the intensity maxima but may be much larger at the intensity minima. Also in Figs. 5 (c) and (d) are the results of simulation (dashed lines). Both simulation and the experiment data are seen to be in good agreement with the theoretical distribution (solid curves) derived in [16].

Since the distribution of phase drift rate is symmetric with respect to zero, we only show the positive half of the distribution. Of interest is the observed off-zero maximum of the distribution for the phase drift at the intensity minima, which implies there is a most probable decoherence rate between the coherence regions.

In Fig. 6a is plotted the probability distribution [23] of the normalized rms time-bandwidth product (tbwp) of the SASE pulses. The distribution average is 1.8. In Fig. 6b, the distribution of the SASE pulse energy is plotted and compared with a gamma distribution with M=1.8. The deviation of the measured distribution from the expected form is believed to be due to experimental limitations described in ref. [23]. The data of ref. [23] showed that the pulses with the highest energy had the lowest tbwp.

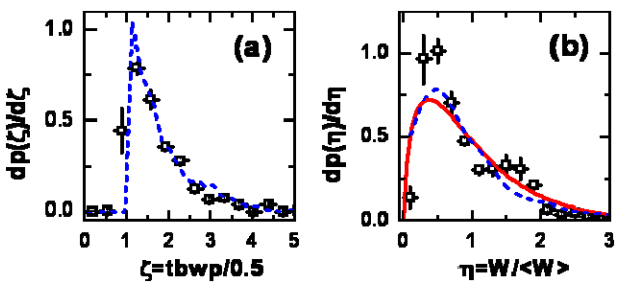

Figure 6: Probability distribution of (**a**) the normalized rms time-bandwidth product, tbwp/0.5= $2\sigma_t\sigma_\omega$, where o.5 is the minimum possible value; and (**b**) the pulse energy. *E*xperiment (symbols); simulation (dashed curves); theory (solid curves). See ref. [23].

CONCLUDING REMARKS

In this paper, we have considered the linear regime before saturation. In the nonlinear saturation regime, SASE is no longer a Gaussian process and analytic treatment is very difficult. A valuable numerical simulation analysis of the statistical behavior in the nonlinear regime can be found in ref. [10,11].

In the SASE FEL, temporal coherence is limited by the short coherence time. Using a laser seed, one can generate a Fourier transform limited pulse. In this regard, high-gain harmonic-generation has been studied experimentally in refs. [25,26]. In the HGHG FEL, the SASE provides a noise limitation [27,28].

ACKNOWLEDGEMENTS

I wish to thank Ilan Ben-Zvi, Robert Gluckstern, Zhirong Huang, Yuelin Li and Li-Hua Yu for their collaborations.

REFERENCES

[1] A. M. Kondratenko, E. L. Saldin, Sov. Phys. Dokl. **24** (12), 986 (1979).
[2] R. Bonifacio, C. Pellegrini, L. M. Narducci, Opt. Commun. **50**, 373 (1984).
[3] J. Galayda et al, Proc. FEL 2009.
[4] Z. Huang and K.-J. Kim, Phys. Rev. ST-AB **10**, 034801 (2007).
[5] J.M. Wang and L.H. Yu, Nucl. Instrum. Meth. **A250**, 484 (1986).
[6] K.J. Kim, Nucl. Instrum. Meth. **A250**, 396 (1986).
[7] L.H. Yu and S. Krinsky, Nucl. Instrum. Methods **A285**, 119 (1989).
[8] S.O Rice, Bell System Technical Journal **24**, 46 (1945). See Section 3.8.
[9] J.W. Goodman, Statistical Optics (John Wiley & Sons, New York, 1985).
[10] E.L. Saldin, E.A. Schneidmiller, M.V. Yurkov, *The Physics of Free Electron Lasers*, Springer-Verlag, Berlin, 2000, Chapter 6.
[11] E.L. Saldin, E.A. Schneidmiller, M.V. Yurkov, Opt. Commun. **148**, 383 (1998).
[12] R. Bonifacio, L. De Salvo, P Pierini, N. Piovella, and C. Pellegrini, Phys. Rev. Lett. **73**, 70 (1994).
[13] K.-J. Kim, *Towards X-Ray Free-Electron Lasers*, ed. by R. Bonifacio and W.A. Barletta (American Institute of Physics, New York, 1997), p.3.
[14] L.H. Yu and S. Krinsky, Nucl. Instrum. Meth. A**407**, 261 (1998).
[15] S. Krinsky and R.L. Gluckstern, Phys. Rev. ST-AB 6:050701 (2003).
[16] S. Krinsky and Y. Li, Phys. Rev. **E73**, 066501 (2006).
[17] M.J. Bastiaans, J. Opt. Soc. Am. A3, 1227 (1986).
[18] L.H. Yu, E. Johnson, D. Li, D. Umstadter, Phys. Rev. **E49**, 4480 (1994).
[19] C.B. Schroeder, C. Pellegrini, S. Reiche, J. Arthur and P. Emma, Nucl. Instrum. Meth. **A483**, 89 (2002).
[20] C.B. Schroeder, C. Pellegrini, S. Reiche, J. Arthur and P. Emma, J. Opt. Soc. Am. **B19** (2002).
[21] S. Krinsky and Z. Huang, Phys. Rev. ST-AB 6:050702 (2003).
[22] Y. Li, S. Krinsky, J. Lewellen, K.J. Kim, V. Sajaev, and S. Milton, Phys. Rev. Lett **91**, 243602 (2003).
[23] Y. Li, S. Krinsky, J. Lewellen and V. Sajaev, Appl. Phys. **B80**, 31 (2004).
[24] R. Trebino et al, Rev. Sck Instrum. **68**, 3277 (1997).
[25] L.H. Yu et al, Science **289** (2000) 932.
[26] L.H. Yu et al, Phys. Rev. Lett. **91**, 074801 (2003).
[27] E.L. Saldin, E.A. Schneidmiller, M.V. Yurkov, Opt. Commun. **202**, 169 (2002).
[28] Z. Huang, Proc. FEL 2006, p130 (2006).